Hindawi
International Journal of Polymer Science
Volume 2020, Article ID 8214549, 10 pages
https://doi.org/10.1155/2020/8214549

Research Article

Mechanical Properties and Enhancement Mechanism of Oil-Well Cement Stone Reinforced with Carbon Fiber Surfaces Treated by Concentrated Nitric Acid and Sodium Hypochlorite

Yongjin Yu,[1] **Jiawen Fu**,[2] **Chi Zhang**,[1] **Fengzhong Qi**,[1] **Ming Li**,[3] **and Junlan Yang**[3]

[1]*CNPC Engineering and Technology Research Institute Co., Ltd., Beijing 102206, China*
[2]*The Second Cementing Branch of CNPC Bohai Drilling Engineering Company Limited, Tianjin 300280, China*
[3]*School of Material Science and Engineering, Southwest Petroleum University, Chengdu 610500, China*

Correspondence should be addressed to Ming Li; swpulm@126.com and Junlan Yang; yjlsoguangyuan@foxmail.com

Received 28 April 2020; Revised 30 September 2020; Accepted 30 October 2020; Published 18 November 2020

Academic Editor: Peng He

In this study, carbon fibers (CFs) were used as toughening materials to improve the mechanical properties of cement stone. The surfaces of the CFs were treated with concentrated nitric acid and sodium hypochlorite to increase the interfacial adhesion between the CFs and the cement. The CFs subjected to surface treatment were evaluated by scanning electron microscopy and infrared analysis to find a significant increase in the number of oxygen-containing groups on the surface. The CFs subjected to surface treatment were added to the cement matrix. The effect of the modified CFs on the mechanical properties of the cement matrix was evaluated by testing the means of mechanical properties. The maximum tensile strength, maximum compressive strength, and ultimate strain of the enhanced cement stone of the CFs treated with sodium hypochlorite increased by 68.2%, 12.0%, and 4.4%, respectively. The maximum tensile strength, maximum compressive strength, and ultimate strain of the enhanced cement stone of the CFs treated with concentrated nitric acid increased by 72.7%, 14.7%, and 4.5%, respectively. The addition of CFs to the cement stone exerted no effect on the type of cement hydration products, as determined by infrared analysis and X-ray diffraction. The toughening mechanism of the modified CFs added to the cement stone was ultimately explored, and the bridging effect, deflection effect, and pull-out effect of cracks were evaluated.

1. Introduction

Oil-well cement stone may exhibit cracking under various external forces within a depth of several hundred or thousand meters underground. The explosion of the perforating bullet, the interaction of stress waves, and the reflection of stress waves may cause the cement ring to rupture [1, 2]. The destruction of the cement ring can severely affect the efficiency of oil recovery. Carbon fibers (CFs) exhibit stable chemical properties and have a large aspect ratio; as such, CFs can efficiently transmit interfacial stress and inhibit the formation and development of cracks, enhancing the strength and durability of the cement stone [3–5].

The surface of a CF is similar to that of a graphite structure, which is inert and water-resistant. These qualities weaken the adhesion of CFs to other substrates, impeding the manufacture of composite materials with excellent performance [6–9]. Accordingly, the surface of the CFs is treated to improve the reactivity and wetness ability of the surface, enhancing the bond strength of the composite interface [10–12].

Various methods commonly used for the surface treatment of CFs include the plasma method, oxidation, chemical grafting, surface coating, and so on [13]. Lee et al. [14] modified the surface of CFs by hydrogen plasma treatment to study its effect on the reinforcement of polyetherimide composites. Through Raman spectroscopy, XPS, FT-IR, and SEM, it is known that the surface roughness and functional group density of CFs were increased by oxyhydrogen plasma treatment. SEM imaging confirmed the enhanced adhesion between CF and PEI, and finally, the tensile properties of the composite at room temperature and high temperature

Table 1: Chemical composition of grade G oil-well cement.

Components	SiO_2	Al_2O_3	Fe_2O_3	CaO	MgO	K_2O	SO_3	MnO_2	Negligible components
Content (wt.%)	22.7	3.39	4.81	65.5	0.9	0.37	1.21	0.09	0.25

(150°C) were improved. Mooseburger-Will et al. [15] functionalized the surface of untreated CFs by low-pressure ammonia plasma treatment and found enhanced concentration of surface nitrogen functionalities and increased surface energy. In addition, plasma treatment does not cause changes in fiber surface topography on the micro- and nanoscales. Arnold et al. [16] oxidized the CF surface at much lower oxidative potentials (+1.75 V), resulting in simultaneous surface modification and oxidation, which led to a substantial increase in interfacial shear strength relative to that of pristine CFs. Kofi et al. [17] used water-soluble sulfonated octaphenyl POSS nanowhiskers to modify the surface of CFs, which improved the chemical uniformity of the surface.

The liquid phase oxidation method [18] mainly uses liquid oxidants to oxidize CFs to change the density and type of surface functional groups. The most commonly used acid is nitric acid. Kim et al. [19] oxidized the surface of rayon-based activated CFs (ACF, KF-1500) with nitric acid and sulfuric acid, respectively. As a result, the total surface acidity of ACFs treated with nitric acid was 10 times greater than that of untreated ACFs and 3.3 times greater than that of ACFs treated with sulfuric acid. In particular, the carboxylic acid and phenol groups of ACFs have been extensively developed by oxidation of nitric acid. The amount of propylamine adsorbed was increased by 17% compared to untreated ACF. Lu et al. [20] used nitric acid to carry out liquid phase oxidation of CFs, and the relationship between liquid phase oxidation time and CF structure was evaluated by LRS, XRD, SEM, and FTIR. As the oxidation time increases, the corrosion increases and the grooves are wider and deeper. Sodium hypochlorite is a strong oxidant, but it treats carbon fiber less. This study is aimed at determining the optimal amount of CFs treated with concentrated nitric acid and sodium hypochlorite blended into cement stone.

2. Experimental Materials and Methods

2.1. Experimental Materials. In this study, G-grade oil-well cement was purchased from Jiahua Special Cement Co., Ltd. The chemical composition and mineral composition are shown in Tables 1 and 2, respectively. Micron-sized CFs were produced from the nanoscience era; Table 3 lists the basic performance parameters of CFs. The other experimental drugs (analytical purity AR) used in this experiment are from the Chengdu Kelong Chemical Reagent Factory with G33S and SXY-2 as the filtrate reducer fluid loss and dispersant, respectively.

2.2. Experimental Process

2.2.1. Surface Cleaning of Carbon Fibers. The surface of the CFs had a binder and thus needed to be cleaned. The CFs were immersed in a beaker containing deionized water,

Table 2: Mineral composition of grade G oil-well cement.

Components	C_3S	C_2S	C_3A	C_4AF
Content (wt.%)	48~65	28~36	1~3	6~14

Table 3: Performance parameters of CFs.

Fiber	Fiber properties	Nature
CF	Fiber length (μm)	10~100
	Fiber diameter (μm)	8~20
	Tensile strength (MPa)	>3300
	Bulk density(g/cm3)	1.76
	Elastic modulus (Gpa)	220

Table 4: Carbon fiber surface treatment.

CF sample	Processing environment	Processing time (min)
P0	Unprocessed	
P1	Sodium hypochlorite 90°C	300
P2	Concentrated nitric acid 75°C	240

Table 5: Cement slurry composition.

Each ingredient	Cement	Water	SXY-2	G33S	CFs
Configuration ratio	1	0.44	0.002	0.01	0.001-0.004

which was then placed in an ultrasonic disperser (BL10-300, Shanghai Bilang Instrument Co., Ltd.) to disperse the CFs for 1 h, followed by degassing using a vacuum pump (not dried after being considered). The CF which was taken care of was placed in another empty beaker into which acetone and absolute ethanol were added at an appropriate ratio of 1 : 1. The beaker was heated in a water bath set to 50°C. The duration of the cleaning time was 24 h. The fiber and liquid were placed on a suction machine and washed with deionized water. The obtained CF was dried in an electric blast drying oven (Type 101, Beijing Zhongxin Weiye Technology Co., Ltd.) at 70°C and dried to constant weight. The sample was then taken out and sealed in a sample bag for use.

2.2.2. Surface Treatment of Carbon Fibers. The CF surface was modified with sodium hypochlorite and concentrated nitric acid, and a blank control was simultaneously set up. During CF oxidation, the constant-temperature water bath (BZKW-4, Beijing Zhongxin Weiye Technology Co., Ltd.) was heated. The surface groups and morphology were analyzed by Fourier transformation infrared spectroscopy (FTIR, Nicolet 6700, American Thermal Power Company) and scanning electron microscopy (SEM, ZEISS EVO MA15, Carl Zeiss Microscopic Imaging Co., Ltd.). Process conditions are shown in Table 4.

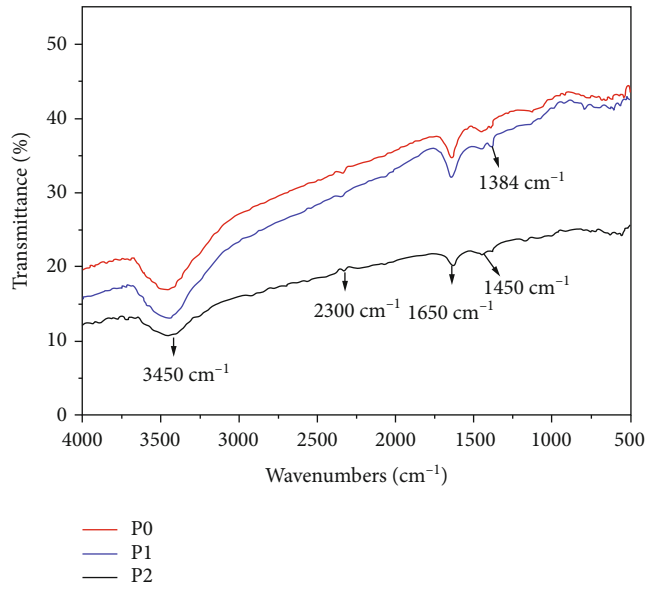

Figure 1: Fourier transform infrared spectroscopy for treated and normal carbon fibers.

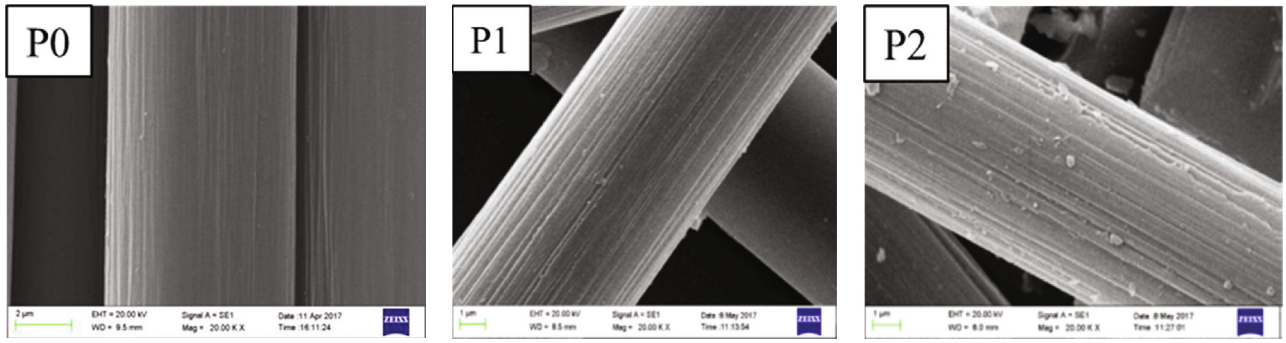

(a) Untreated CFs (b) CFs treated with sodium hypochlorite (c) CFs treated with concentrated nitric acid

Figure 2: Scanning electron micrographs of carbon fibers.

2.2.3. Preparation of Cement Stone. Cement slurry was prepared based on the quality of the cement. Each component was added at a certain proportion (mass fraction) (Table 5).

The CF content was set to 0, 0.1%, 0.2%, 0.3%, and 0.4%. The CFs were dispersed and placed in a high-speed frequency conversion stepless speed mixer (GJS-B12K, Qingdao Tongchun Petroleum Instrument Co., Ltd.) for use. Each component was weighed by a precision electronic balance (JJ300, American Shuangjie Brothers Group Co., Ltd.). Specifically, 300 g cement was used. Other remaining components were weighed proportionally. The weighed ingredients and CF were added to the cement and mixed thoroughly. The stirred cement was then added to the water for artificial mixing, stirred manually, and stirred with a high-speed mixer (5000 rpm) for 2 min to ensure that the ingredients were evenly dispersed. After stirring, 1-2 drops of a defoamer were added into the cement, and the mixture was stirred to form a cement slurry. The bubbles subsequently disappeared. Finally, different formulations of cement slurry were poured into various standard molds to maintain different days in a constant temperature water bath at 60°C.

2.2.4. Testing of Mechanical Properties of Cement Stone. Different samples of cement stone were prepared using different molds to evaluate the different mechanical properties of the cement stone. The cement slurry was cast into a rectangular mold ($50.8 \times 50.8\,\text{m} \times 50.8\,\text{mm}^3$) and a cylindrical mold ($\Phi 50.0 \times 25.0\,\text{mm}^3$) to test its compressive strength and tensile strength by using electronic hydraulic testing machines (Haizhi Technology Co. Ltd., Beijing, China) at a crosshead speed of 600 N/s. Triaxial stress-strain curves were generated on a triaxial rock-testing system (INT-2200, GCTS) by using a rectangular specimen ($40.0 \times 40.0 \times 160.0\,\text{mm}^3$) cured at 60°C for 7 d. Triaxial testing was conducted under 20.7 MPa confining pressure and 60°C.

2.2.5. Microstructural Analysis. X-ray diffraction (Shimadzu, XRD-7000 Japan) with Cu-K radiation (=0.15406 nm) was used for phase analysis of the cement stone, including blank cement samples and CF-reinforced cement samples. The sample was a dry powdery substance with a fineness of about 45 microns. The scan range was changed from 10°C to 60°C, with a step size of 0.02. The infrared

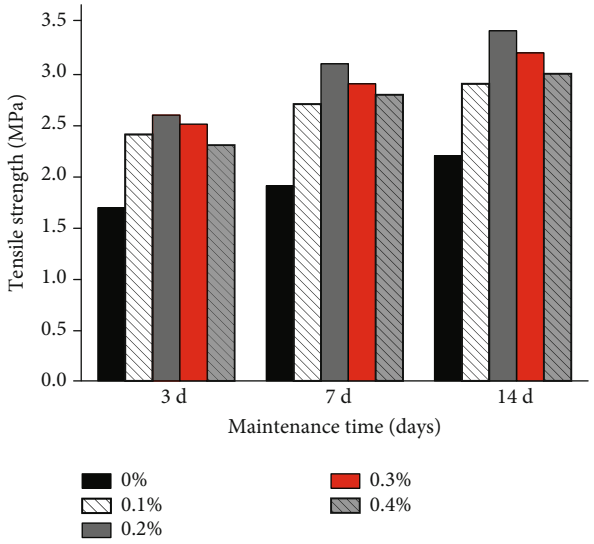

(a) Tensile strength of pure cement stone and untreated CF-reinforced cement stone

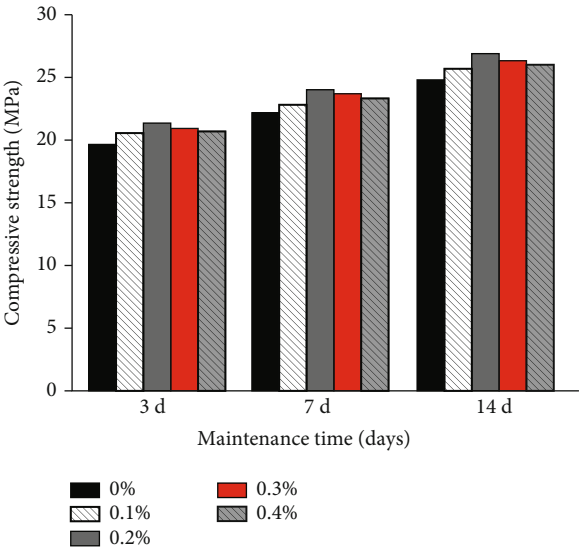

(b) Compressive strength of pure cement stone and untreated CF-reinforced cement stone

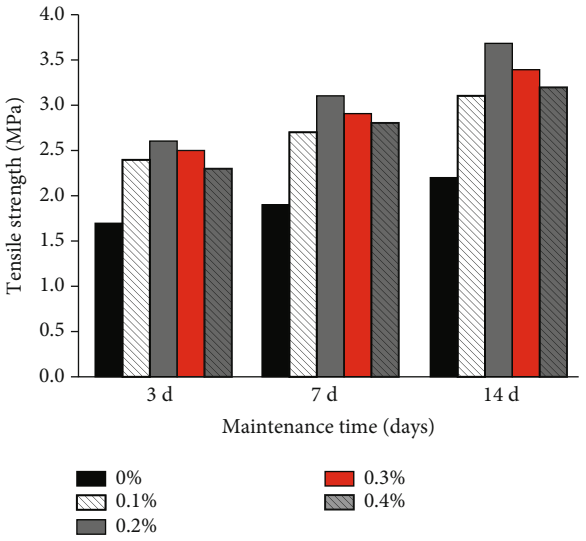

(c) Tensile strength of pure cement stone and CF-reinforced cement stone added with sodium hypochlorite

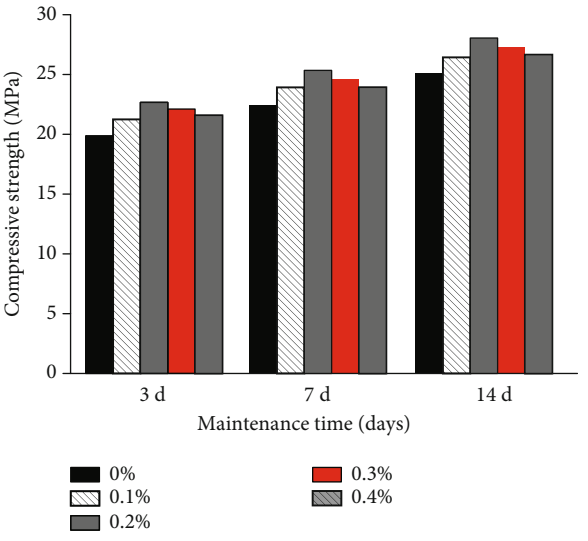

(d) Compressive strength of pure cement stone and CF-reinforced cement stone treated with sodium hypochlorite

Figure 3: Continued.

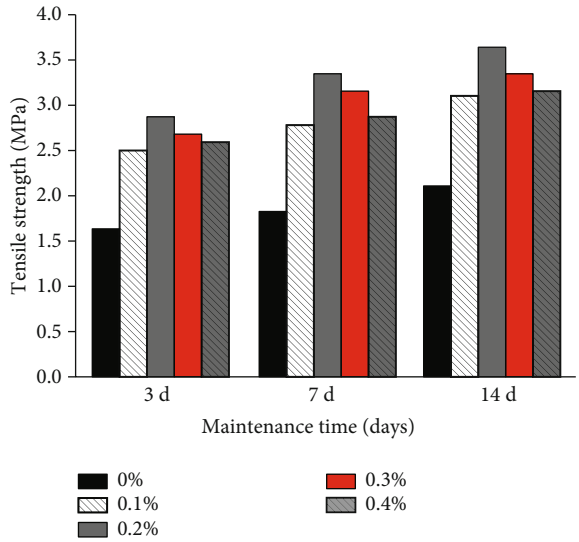

(e) Tensile strength of pure cement stone and CF-cement-reinforced stone treated with concentrated nitric acid

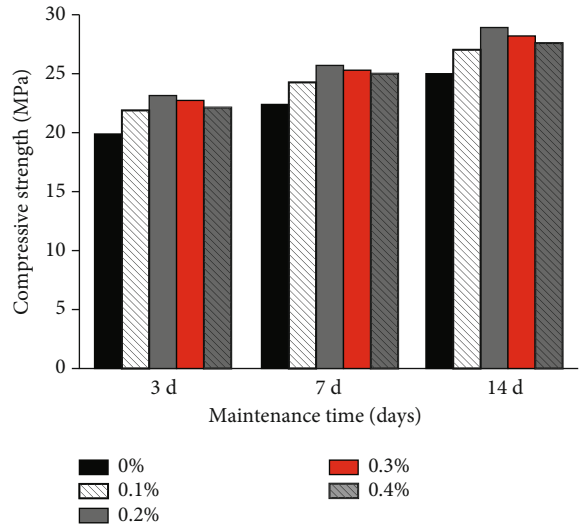

(f) Compressive strength of pure cement stone and CF-reinforced cement stone treated with concentrated nitric acid

Figure 3: Compressive strength and tensile strength of cement stone.

Table 6: Comparison of mechanical strength between carbon fiber-reinforced cement stone and pure cement stone.

CF type added	Content of CF (%)	Compressive strength increase (%)	Tensile strength increase (%)
P0	0.2%	8.4%	40.9%
P1	0.2%	12.0%	68.2%
P2	0.2%	14.7%	72.7%

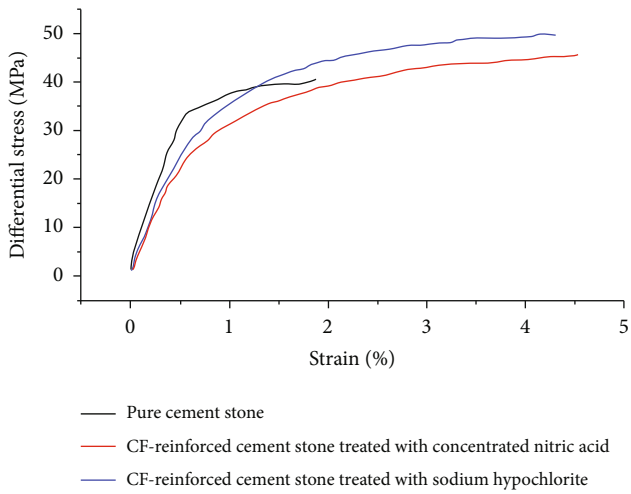

Figure 4: Triaxial stress-strain curves of cement stone.

spectrometer (NICOLET-6700, American Thermo Fisher Scientific Co., Ltd.) was used to evaluate changes in the functional groups and chemical bonds before and after toughening of the cement stone. The dried 1 mg sample was finely ground with 100 mg pure KBr, placed in a

Table 7: Mistrial testing results for cement stone.

CF type added	Content of CF (%)	Peak stress (MPa)	Elasticity modulus (MPa)	Peak stain (%)
P0	0	40.8	6645	1.8%
P1	0.2%	49.6	4962	4.4%
P2	0.2%	45.8	4907	4.5%

mold, and pressed into a transparent film for measurement. The instrument parameters were as follows: spectral range, 4000-500 cm^{-1}; resolution, >0.1 cm^{-1}; and wavenumber accuracy, >0.01 cm^{-1}. To determine the crack propagation behavior, the fracture of pure cement stone and CF-reinforced cement stone was observed by SEM (JEOL JSM-6510LV, Japan). The working voltage was 5 kV, and the emission current was 10 μm.

3. Results and Discussion

3.1. Results of Carbon Fiber Surface Treatment. The FTIR spectra of the normal CF and the treated CF samples, except that of the CF treated with concentrated nitric acid, showed an absorption peak of -NO_2 at 1384 cm^{-1} (Figure 1). No significant difference in the positions of the other peaks was found, indicating that the treatment of CFs only slightly affected the chemical composition. The same peaks were observed at 3450, 2300^{-1}, 1650^{-1}, and 1450 cm^{-1}, corresponding to -OH, C≡C, C=O, and-C-O, respectively [21, 22]. The peak intensity of the treated CF increased significantly at 3450 and 1650 cm^{-1}, indicating an increase in the oxygen-containing functional group on the surface of CFs.

As shown in Figure 2, the ravines on the surface of the CFs treated with concentrated nitric acid and sodium hypochlorite were deeper and wider than those of the normal

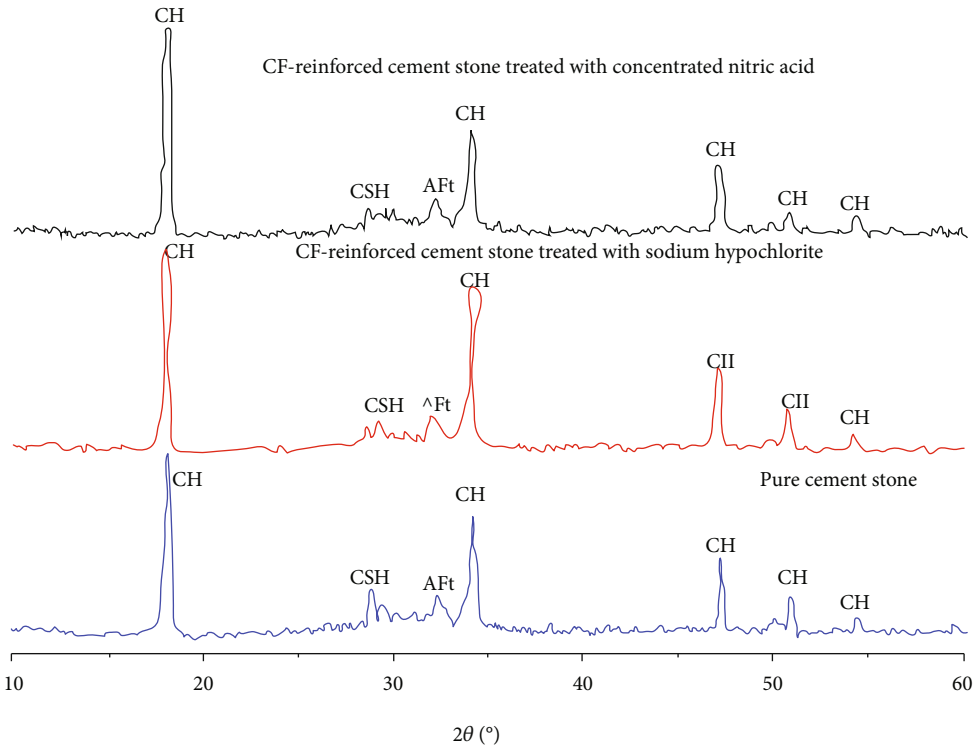

Figure 5: XRD pattern of cement stone with 0.2% CF cured for 7 days.

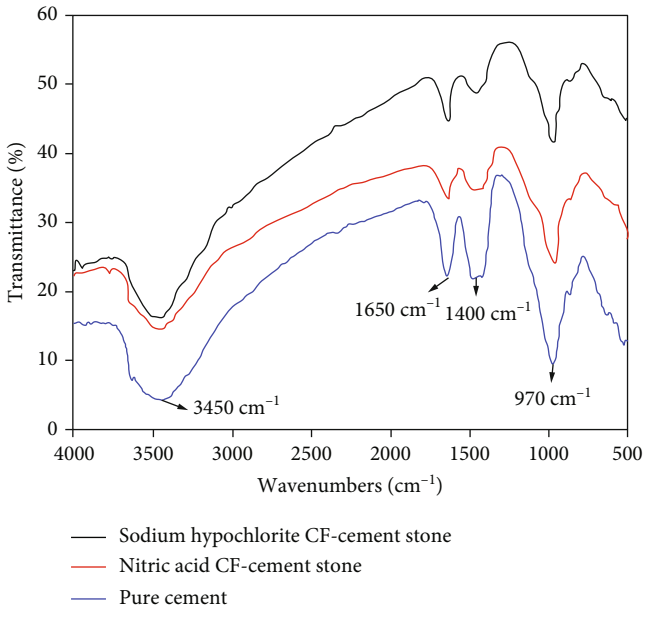

Figure 6: FTIR of cement stone with 0.2% CF for 7 days.

CFs. These gullies formed on the surface of the fibers increased the specific surface area of the CFs. The contact area was increased with the cement stone, which can increase the interface bonding force. Compared with the CFs treated with sodium hypochlorite, the CFs treated with concentrated nitric acid have more and deeper ravines on the surface. This is because concentrated nitric acid is more corrosive and more destructive to the surface of CFs.

3.2. Mechanical Properties of Cement Stone. Figure 3 presents various CFs with a reinforcing effect on the cement stone. The optimum blending amount of the CFs in various treatment methods was 0.2%. When the CF content exceeded 0.2%, the reinforcing effect tended to decrease, but the mechanical properties were still greater than those of pure cement stone, which may be attributed to the agglomeration of CF, so the CF content should have a suitable value [23–25]. The reinforcing effect became more apparent as the curing time increased, which due to the increase in hydration time contributes to the bonding of the CF to the cement matrix [23]. The CF-reinforced cement stone treated with concentrated nitric acid exhibited the best reinforcing effect, followed by the CF-reinforced cement stone treated with sodium hypochlorite; untreated carbon fiber also had certain enhancement effect on cement stone, but the effect was not as good as the former two; the details are listed in Table 6.

Figure 4 presents the triaxial stress-strain curves of cement stone, and the results are listed in Table 7. The CF-cement-reinforced stone treated with sodium hypochlorite increased the ultimate strain and ultimate stress of the cement stone by 144.4% and 21.6% compared to pure cement stone, respectively, and the elastic modulus decreased by 25.3%. The CF-cement-reinforced stone treated with nitric acid increased the ultimate strain and ultimate stress of cement stone by 12.2% and 150%, respectively, and the elastic modulus decreased by 26.2%. CFs were added to the brittle cement stone, and the toughness and ductility of the cement stone are greatly improved [25]. The toughening effect of CFs treated with nitric acid on cement stone is better than that of CFs treated with sodium hypochlorite.

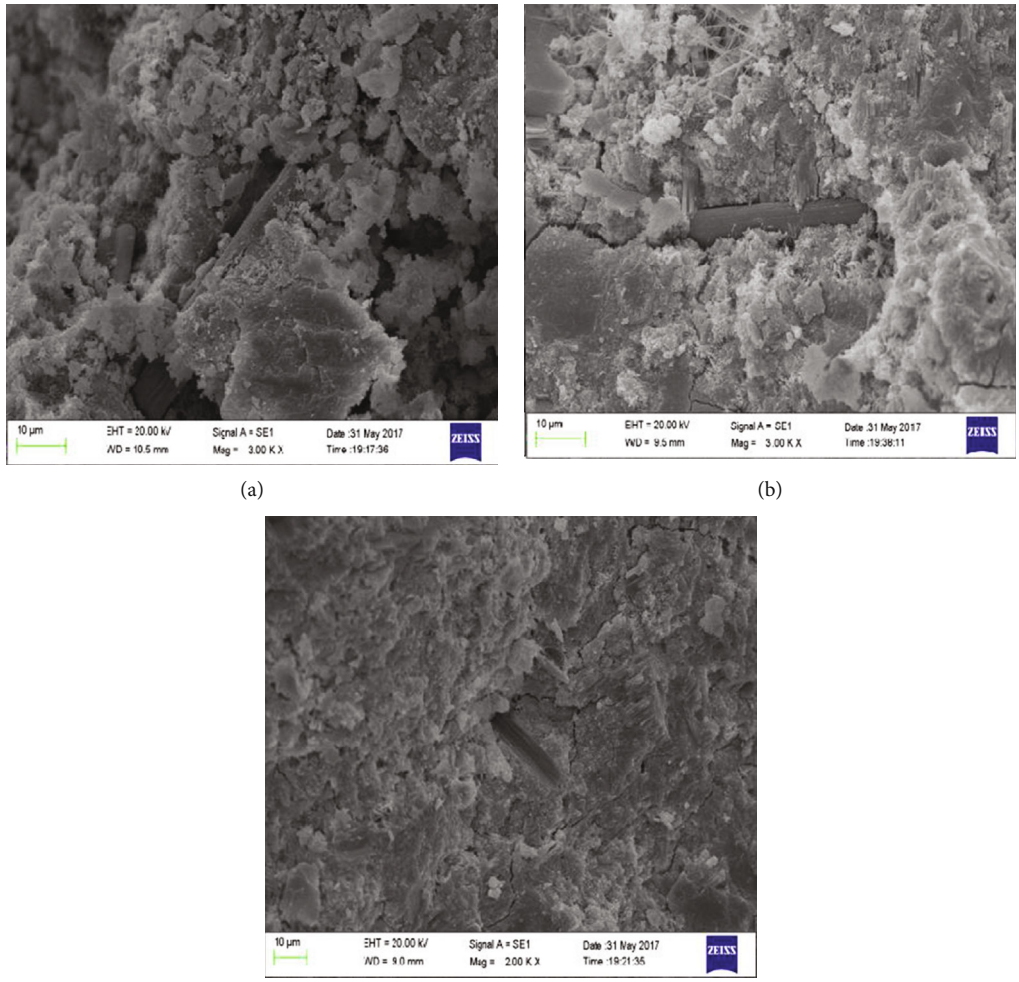

Figure 7: SEM image of cement stone after curing for 7 days with 0.2% CF addition.

3.3. Hydration Products of Cement Stone. For the blank group, XRD spectra of the CF-cement stone system treated with concentrated nitric acid and concentrated sodium hypochlorite are shown in Figure 5. It can be seen that the hydration products in samples consisted of C-S-H (calcium silicate hydrate), C-H (calcium hydroxide), and AFt (calcium gangue). The results indicate that the type of hydration products was not changed due to the addition of CF. Compared with the samples treated with sodium hypochlorite, the C-H diffraction peaks in the samples treated with concentrated nitric acid are weaker. The reason is that CF reacts with C-H to form C-S-H, which reduces the layered C-H content and improves the strength of the cement paste. This explains why the compressive strength, tensile strength, and ultimate strain of the cement paste have been improved after adding CF treated with concentrated nitric acid [26].

Figure 6 presents the infrared spectra of the CF-reinforced cement stone treated with nitric acid, CF-reinforced cement stone treated with sodium hypochlorite, and pure cement stone. The infrared spectra between them were basically similar, the group type did not change, and no new functional groups were formed. As shown in the figure, the peak at 3450 cm^{-1} is the hydroxyl group (-OH) in the cement calcium hydroxide phase [27, 28], and the peak at 970 cm^{-1} on the right side corresponds to the characteristic peak of Si-O tetrahedron $[SiO_4]^{4-}$ in CSH. The peak at 1400^{-1} corresponds to CO_3^{2-} of calcium vanadium, and the peak at 1650^{-1} corresponds to the hydroxyl group in CFs and water [29]. The addition of CF to the cement stone only slightly affects the type of cement hydration products, as determined by XRD and FTIR analyses [30, 31].

3.4. Mechanism of Carbon Fiber-Reinforced Cement Stone. The mechanism of carbon fiber-reinforced cement paste mainly includes three aspects. In cement paste, the carbon fiber can make a crack bridging effect, crack deflection effect, and crack extraction effect. The cement stone will generate a large number of microcracks in the initial stage of the external load. When the crack extends to the CF, it will bear the load of the part of the cement stone and bridge the opposite sides of the crack due to higher mechanical properties of CFs (Figure 7(a)), so the crack needs to consume more energy to propagate further [32, 33]. When the crack further expands, the energy of the extended crack is not enough to

cause the CF to break, and the crack deviates from the original route and continues to expand along the interface where the bonding force is not strong, which is manifested by the fact that the shape of the crack is curved (Figure 7(b)), thereby delaying the crack propagation [34–36]. When the cement stone is subjected to a sustained load, the bonding strength between the CF and the cement stone will not be sufficient to prevent the crack from expanding, and the CF will be peeled out of the cement stone. Figure 7(c) shows the holes left by the CF pulled out of the cement. This process also dissipates a lot of energy [37, 38]. The stronger the bonding strength between CF and the cement stone, the more energy is dissipated, so it can be well explained that the bonding strength between CF and cement stone is an important factor affecting the performance of the cement stone. The use of concentrated nitric acid and sodium hypochlorite to treat CFs can increase the surface area of the carbon fiber, thereby enhancing the bonding force with the cement stone.

As previously mentioned, the liquid phase oxidation has three effects [39, 40]: (1) the surface of the CF is oxidized to a certain extent, and the number of oxygen-containing functional groups on the surface is increased, which increases the chemical interaction between the surface of the CF and the cement matrix; (2) the ratio of different functional groups on the surface of the CF changes, improving the wettability of the cement matrix on the surface of the CF; (3) surface treatment causes a certain etching on the surface of the CF to improve the physical hinge interaction between the surface of the CF and the cement matrix. The carbon fiber is treated and better combined with the cement matrix, so the enhanced toughening effect of the treated carbon fiber is greater than that of the carbon fiber without any treatment, and the CF surface treated by the nitric acid is the best. Studying the surface treatment of CF is very meaningful as a cement-reinforced phase.

4. Conclusions

(1) For the cement stone, the optimal amount of CF is 0.2%; surface treatment of the CFs with concentrated nitric acid and sodium hypochlorite changes the surface morphology of the CF to a certain extent. The CFs treated with concentrated nitric acid exert a better reinforcement effect on the cement stone, compared with the CFs treated with sodium hypochlorite. The CFs subjected to surface treatment with concentrated nitric acid increase the tensile strength of the cement stone by 72.7% and the compressive strength by 14.2% when the CF content is optimal

(2) The results of the triaxial test indicate that the differential stress of the modified cement stone is increased by about 7 MPa relative to that of pure cement. The ultimate strain is about twice that of the pure cement stone, but the elastic modulus is reduced by about 1700 MPa

(3) The surface of CFs treated with concentrated nitric acid has more and more obvious gully. The interface bonding force with cement stone is greater, with better tensile strength, compressive strength, and ultimate strain

(4) CFs exert no effect on the hydration products of the cement stone

(5) The mechanism of carbon fiber-reinforced cement stone is mainly crack bridging, crack deflection, and crack extraction

Data Availability

The [data type] data used to support the findings of this study are included within the article.

Additional Points

Highlights. The surfaces of the carbon fibers were treated with concentrated nitric acid and sodium hypochlorite to increase the interfacial adhesion between the carbon fibers, and the cement carbon fibers were used to enhance the oil-well cement stone The toughening mechanism of the carbon fiber-reinforced oil-well cement stone was explored in detail.

Conflicts of Interest

The authors declare that there are no conflicts of interest regarding the publication of this paper.

Acknowledgments

The authors would like to acknowledge the financial support by CNPC Science and Technology Project (2019A-3910) and the National Natural Science Foundation of China (51874254).

References

[1] M. Li, S. Deng, Y. Yu, J. Jin, Y. Yang, and X. Guo, "Mechanical properties and microstructure of oil well cement stone enhanced with tetra-needle like ZnO whiskers," *Construction and Building Materials*, vol. 135, pp. 59–67, 2017.

[2] C. Zhang, Y. Song, W. Wang, X. Guo, and H. Li, "The influence of sulfonated asphalt on the mechanical properties and microstructure of oil well cement paste," *Construction and Building Materials*, vol. 132, pp. 438–445, 2017.

[3] M. Li, M. Liu, Y. Yang, Z. Li, and X. Guo, "Mechanical properties of oil well cement stone reinforced with hybrid fiber of calcium carbonate whisker and carbon fiber," *Petroleum Exploration and Development*, vol. 42, no. 1, pp. 104–111, 2015.

[4] M. Li, Y. Yang, M. Liu, X. Guo, and S. Zhou, "Hybrid effect of calcium carbonate whisker and carbon fiber on the mechanical properties and microstructure of oil well cement," *Construction and Building Materials*, vol. 93, pp. 995–1002, 2015.

[5] M. Hambach, H. Möller, T. Neumann, and D. Volkmer, "Carbon fibre reinforced cement-based composites as smart floor heating materials," *Composites Part B: Engineering*, vol. 90, pp. 465–470, 2016.

[6] D. Semitekolos, P. Kainourgios, C. Jones, A. Rana, E. P. Koumoulos, and C. A. Charitidis, "Advanced carbon fibre composites via poly methacrylic acid surface treatment; surface

analysis and mechanical properties investigation," *Composites Part B: Engineering*, vol. 155, pp. 237–243, 2018.

[7] J. Moosburger-Will, M. Bauer, E. Laukmanis et al., "Interaction between carbon fibers and polymer sizing: influence of fiber surface chemistry and sizing reactivity," *Applied Surface Science*, vol. 439, pp. 305–312, 2018.

[8] S. J. Park, Y. Jung, and S. Kim, "Effect of fluorine–oxygen mixed gas treated graphite fibers on electrochemical behaviors of platinum–ruthenium nanoparticles toward methanol oxidation," *Journal of Fluorine Chemistry*, vol. 144, no. 36, pp. 124–129, 2012.

[9] W. Song, A. Gu, G. Liang, and L. Yuan, "Effect of the surface roughness on interfacial properties of carbon fibers reinforced epoxy resin composites," *Applied Surface Science*, vol. 257, no. 9, pp. 4069–4074, 2011.

[10] X. Fu, W. Lu, and D. D. L. Chung, "Improving the bond strength between carbon fiber and cement by fiber surface treatment and polymer addition to cement mix," *Cement and Concrete Research*, vol. 26, no. 7, pp. 1007–1012, 1996.

[11] E. Laukmanis, B. Brück, M. Bauer, J. Moosburger-Will, and S. R. Horn, "Wetting behavior of carbon fibers: influence of surface activation and sizing type," *Key Engineering Materials*, vol. 742, pp. 457–462, 2017.

[12] O. Abdel Gawad, M. H. Abou Tabl, Z. Abdel Hamid, and S. F. Mostafa, "Electroplating of chromium and Cr-carbide coating for carbon fiber," *Surface & Coatings Technology*, vol. 201, no. 3-4, pp. 1357–1362, 2006.

[13] A. Kafi, M. Huson, C. Creighton et al., "Effect of surface functionality of PAN-based carbon fibres on the mechanical performance of carbon/epoxy composites," *Composites Science and Technology*, vol. 94, pp. 89–95, 2014.

[14] E. Lee, C. H. Lee, Y. S. Chun, C. J. Han, and D. S. Lim, "Effect of hydrogen plasma-mediated surface modification of carbon fibers on the mechanical properties of carbon-fiber-reinforced polyetherimide composites," *Composites Part B: Engineering*, vol. 116, pp. 451–458, 2017.

[15] J. Moosburger-Will, E. Lachner, M. Löffler et al., "Adhesion of carbon fibers to amine hardened epoxy resin: influence of ammonia plasma functionalization of carbon fibers," *Applied Surface Science*, vol. 453, pp. 141–152, 2018.

[16] C. L. Arnold, K. M. Beggs, D. J. Eyckens, F. Stojcevski, L. Servinis, and L. C. Henderson, "Enhancing interfacial shear strength via surface grafting of carbon fibers using the Kolbe decarboxylation reaction," *Composites Science and Technology*, vol. 159, pp. 135–141, 2018.

[17] A. Kafi, Q. Li, T. Chaffraix, J. Khoo, T. Gengenbach, and K. J. C. Magniez, "Surface treatment of carbon fibres for interfacial property enhancement in composites via surface deposition of water soluble POSS nanowhiskers," *Polymer*, vol. 137, pp. 97–106, 2018.

[18] M. S. Ahmad, M. K. Abdelazeez, A. Zihlif, E. Martuscelli, G. Ragosta, and E. Scafora, "Some properties of nickel-coated carbon fibre-polypropylene composite at microwave frequencies," *Journal of Materials Science*, vol. 25, no. 7, pp. 3083–3088, 1990.

[19] B. K. Kim, B. H. Yang, and S. K. Ryu, "Propylamine adsorption characteristics of surface-treated activated carbon fibers with nitric acid and sulfuric acid," *Korean Chemical Engineering Research*, vol. 42, no. 5, pp. 551–557, 2004.

[20] W. B. Lu, C. G. Wang, H. Yuan, and X. Y. Hu, "Liquid-phase oxidation modification of carbon fiber surface," *Advanced Materials Research*, vol. 430-432, pp. 2008–2012, 2012.

[21] K. Kannan, D. Radhika, M. P. Nikolova, V. Andal, K. K. Sadasivuni, and L. S. Krishna, "Facile microwave-assisted synthesis of metal oxide CdO-CuO nanocomposite: photocatalytic and antimicrobial enhancing properties," *Optik*, vol. 218, p. 165112, 2020.

[22] K. Kannan, D. Radhika, A. S. Nesaraj, M. Wasee Ahmed, and R. Namitha, "Cost-effective method of Co-doped rare-earth-based ceria (Y-CGO) nanocomposite as electrolyte for LT-SOFCs using C-TAB as surfactant," *Materials Research Innovations*, vol. 24, no. 7, pp. 414–421, 2020.

[23] X. Yan and S. Cao, "Structure and interfacial shear strength of polypropylene-glass fiber/carbon fiber hybrid composites fabricated by direct fiber feeding injection molding," *Composite Structures*, vol. 185, pp. 362–372, 2018.

[24] S. P. Yap, C. H. Bu, U. J. Alengaram, K. H. Mo, and M. Z. Jumaat, "Flexural toughness characteristics of steel–polypropylene hybrid fibre-reinforced oil palm shell concrete," *Materials and Design*, vol. 57, pp. 652–659, 2014.

[25] L. Restuccia and G. A. Ferro, "Promising low cost carbon-based materials to improve strength and toughness in cement composites," *Construction and Building Materials*, vol. 126, pp. 1034–1043, 2016.

[26] C. Zhang, J. Cai, H. Xu, X. Cheng, and X. Guo, "Mechanical properties and mechanism of wollastonite fibers reinforced oil well cement," *Construction and Building Materials*, vol. 260, p. 120461, 2020.

[27] K. Kannan, D. Radhika, S. Vijayalakshmi, K. K. Sadasivuni, A. A. Ojiaku, and U. Verma, "Facile fabrication of CuO nanoparticles via microwave-assisted method: photocatalytic, antimicrobial and anticancer enhancing performance," *International Journal of Environmental Analytical Chemistry*, pp. 1–14, 2020.

[28] K. Kannan, D. Radhika, A. S. Nesaraj, V. Revathi, and K. K. Sadasivuni, "A simple chemical precipitation of ceria based (Sm doped-CGO) nanocomposite: structural and electrolytic behaviour for LT-SOFCs," *SN Applied Sciences*, vol. 2, no. 7, 2020.

[29] K. Kannan, D. Radhika, M. P. Nikolova, K. K. Sadasivuni, and N. R, "Structural and functional properties of rare earth-based (NiO-CGO) nanocomposite produced by effective multiple doping approach via co-precipitation," *Materials Technology*, pp. 1–12, 2020.

[30] K. Kannan, D. Sivasubramanian, P. Seetharaman, and S. Sivaperumal, "Structural and biological properties with enhanced photocatalytic behaviour of CdO-MgO nanocomposite by microwave-assisted method," *Optik*, vol. 204, p. 164221, 2020.

[31] V. Revathi and K. Karthik, "Physico-chemical properties and antibacterial activity of Hexakis (Thiocarbamide) Nickel(II) nitrate single crystal," *Chemical Data Collections*, vol. 21, p. 100229, 2019.

[32] M. Li, M. He, Y. Yu, S. Deng, and X. Guo, "Mechanical properties and microstructure of oil-well cement stone enhanced with submicron SiC whiskers," *Journal of Adhesion Science and Technology*, vol. 33, no. 1, pp. 50–65, 2018.

[33] S. S. Kutanaei and A. J. Choobbasti, "Triaxial behavior of fiber-reinforced cemented sand," *Journal of Adhesion Science and Technology*, vol. 30, no. 6, pp. 579–593, 2015.

[34] D. H. Kim and C. G. Park, "Strength, permeability, and durability of hybrid fiber-reinforced concrete containing styrene butadiene latex," *Journal of Applied Polymer Science*, vol. 129, no. 3, pp. 1499–1505, 2013.

[35] M. Cao, C. Zhang, and J. Wei, "Microscopic reinforcement for cement based composite materials," *Construction and Building Materials*, vol. 40, pp. 14–25, 2013.

[36] K. T. Faber and A. G. Evans, "Crack deflection processes—II. Experiment," *Acta Metallurgica*, vol. 31, no. 4, pp. 577–584, 1983.

[37] M. Alam, J. P. Parmigiani, and J. J. Kruzic, "An experimental assessment of methods to predict crack deflection at an interface," *Engineering Fracture Mechanics*, vol. 181, pp. 116–129, 2017.

[38] E. Breitbarth and M. Besel, "Fatigue crack deflection in cruciform specimens subjected to biaxial loading conditions," *International Journal of Fatigue*, vol. 113, pp. 345–350, 2018.

[39] C. Kayadelen, T. Ö. Önal, and G. Altay, "Experimental study on pull-out response of geogrid embedded in sand," *Measurement*, vol. 117, pp. 390–396, 2018.

[40] K. Matsumoto, H. Yamaguchi, and K. Nagai, "Fatigue pull-out failure of deformed bars in concrete under the effect of liquid water," *Cement and Concrete Composites*, vol. 91, pp. 198–208, 2018.